Int. J. Electrochem. Sci., 15 **(2020)** 7575 – 7584, doi: 10.20964/2020.08.29

International Journal of ELECTROCHEMICAL SCIENCE
www.electrochemsci.org

Synthesis of Iron(III) Tetracarboxyl–Phthalocyanine Sensitized Nano TiO_2 Composite as Photoelectrochemical Hydroquinone Sensor

Yuxia Liu

Department of Physics and Electronic Engineering, Guangxi Normal University for Nationalities, Chongzuo 532200, China
E-mail: liuyuxiayx@163.com

Received: 9 March 2020 / *Accepted:* 15 May 2020 / *Published:* 10 July 2020

In this work, a simple photoelectrochemical (PEC) sensor was developed using anatase TiO_2 nanoparticles sensitized with iron(III) tetracarboxyl phthalocyanine ($FeC_4Pc@TiO_2$) for detection of hydroquinone (HQ). The $FeC_4Pc@TiO_2$ composite shows excellent photoelectrochemical activity under visible-light illumination compared with pure anatase TiO_2 nanoparticles and pure FeC_4Pc. After adding HQ, the photocurrent of the $FeC_4Pc@TiO_2$-modified indium tin oxide electrode ($FeC_4Pc@TiO_2$/ITO) was significantly enhanced, which was attributed to the life improvement of the electron–hole pairs. The sensor was developed based on the enhanced photocurrent response signal. The photocurrent response signal is linear with the concentration of HQ ranging from 0.2 μM to 78 μM, with a detection limit of 0.078 μM (S/N=3) under the optimal conditions. The PEC sensor showed high sensitivity, low cost, and wide linearity range and was successfully employed in the analysis of real water samples, with recoveries between 99.7%–101.7%.

Keywords: Photoelectrochemical sensor; TiO_2 nanoparticles; Iron(III) Tetracarboxyl Phthalocyanine; hydroquinone

1. INTRODUCTION

Photoelectrochemical (PEC) sensor based on electrochemical (EC) sensor is a novel and dynamically developing technology for detection and analysis. The PEC sensor combines optical and EC technologies and possesses the advantages of simple operation, fast response, low cost, and easy miniaturization [1-2]. Moreover, the sensor presents the characteristics of low background signal and high sensitivity due to the efficient separation between the excitation source and the detector apparatus of the response signal [3]. The PEC sensor has received extensive research attention as a highly promising analytical method for detection of various analytes, such as environmental pollutants [4],

pesticides [5], clinical drugs [6-8], biomolecules [9], and heavy metal ions [10].

The strength of response signal depends on the catalytic activity and photoelectric conversion efficiency of photoelectric active materials, which thus play a crucial role in construction of PEC sensors. In recent years, inorganic semiconductors, including metallic oxide [11,12], quantum dots [13], carbon-based nanomaterials [14], and metal nanoparticles [15], are widely applied in the field of PEC sensing due to their superior photocatalytic activity. Among these materials, TiO_2 is recognized as one of the most attractive semiconductor for development of PEC sensors owing to its low toxicity, excellent biocompatibility, high photochemical stability, and catalytic efficiency [16]. However, pure anatase TiO_2 with wide band gap (~3.2 eV) only absorbs ultraviolet light, which limits its application in PEC sensors [17]. In addition, the rapid recombination of the photoexcited electron–hole pairs is faster than the time required for these carriers to react with adsorbed molecules [18]. To overcome these disadvantages, researchers have proposed various modification methods, including dye sensitization [19], metal and non-metal load [20], or coupling with a narrow band gap semiconductor [21] for improving the visible-light response of TiO_2 nanoparticles.

Phthalocyanine derivatives are organic optoelectronic molecules with highly delocalized conjugated systems and are used as sensitizers. These derivatives have strong absorption to visible light and perfect electron injection and electron transfer ability owing to their distinct structure [22-24]. Furthermore, the structural flexibility of these derivatives allows them to be modified with functional groups [25]. However, single phthalocyanine used as a photoelectric conversion layer generates weak photocurrent and thus needs to be compounded with other conductive materials. In recent years, studies of metal phthalocyanine and TiO_2 composites have received increasing attention due to the strong electronic coupling effect and mainly focus on development of PEC sensors [26,27], photoinduced degradation of organic compounds [28], and photodynamic therapy [29].

Hydroquinone (HQ) plays a key role in many fields, including photographic development, dyes, rubber production, and paper manufacturing [30]. HQ is difficult to degrade and is considered an important exogenous pollutant in the aquatic environment. In addition, the toxicity of HQ may cause possible health problems, including skin and nose irritation, dizziness, coma, tinnitus, and breathing difficulties, to humans and animals [31]. Therefore, an accurate, rapid, and reliable method for HQ detection is of great practical significance. To date, various technologies have been exploited to detect HQ; these technologies include chemiluminescent analysis [32], high-performance liquid chromatography (HPLC) [33], gas chromatography–mass spectrometry (GC-MS) [34], EC sensors [35], and PEC sensors [36]. Among these technologies, PEC sensor has been extensively studied because it exhibits the advantages of optical and EC sensors, including miniaturization capability, noticeable sensitivity, and simple integration.

In this work, FeC_4Pc was synthesized successfully and a novel PEC sensor based on $FeC_4Pc@TiO_2$ composite was developed for detection of HQ. The fabricated PEC sensor showed favorable performance in the detection of HQ and demonstrated appreciable stability, high sensitivity, and excellent selectivity under visible-light illumination. Hence, this sensor has great potential and is expected to become a universal detection tool in the field of environmental monitoring.

2. MATERIALS AND METHODS

2.1 Materials and reagents

Indium tin oxide (ITO) thin film-coated glass slices were acquired from Xiangcheng Technology Co., Ltd. (Shenzhen, China). HQ, anatase TiO_2 nanoparticles, trimellitic anhydride, ferric chloride, and urea were purchase from Aladdin Biochemical Technology Co., Ltd. (Shanghai, China). Dimethyl sulfoxide (DMSO) and other unmentioned chemicals were obtained from Kelong Chemical Reagent Plant (Chengdu, China). Phosphate buffer saline (PB, 0.1 M) was prepared using NaH_2PO_4 and Na_2HPO_4. All chemicals used in this work were of analytical grade.

2.2 Apparatus

A PEAC 200A photoelectric alignment collimator (Tjaida Instrument Co., Tianjin, China) with a 10 W light-emitting diode (LED) was used as the irradiation source. Photocurrent signals were acquired by a CHI760E electrochemical workstation (Chenhua Instrument Co., Shanghai, China) with three-electrode system. The modified ITO electrode was employed as the working electrode. A Pt wire was used as the counter-electrode, and a saturated Ag/AgCl electrode was used as the reference electrode. Ultraviolet-visible (UV-Vis) spectra were recorded on a UV-6100S spectrometer (Metash Instruments Co., Ltd., Shanghai, China) within 200 nm to 800 nm. Fourier transform infrared (FTIR) spectra were recorded on a Spectrum65 spectrophotometer (Perkin Elmer, Santa Clara, CA, USA).

2.3 Synthesis of iron(III) tetracarboxyl phthalocyanine

Iron(III) tetracarboxyl phthalocyanine (FeC_4Pc) was prepared according to a previously reported method [37]. The mixture of 9.60 g of trimellitic anhydride, 4.87 g of iron chloride, 30.00 g of urea, 0.2 g of ammonium molybdate, and 120 mL of kerosene was gradually heated and maintained at 198 °C for 2.5 h with stirring under reflux. The dark green foamy solid was stirred, filtered, and washed several times with mineral ether, methyl alcohol, deionized water, and hot ethanol. Iron(III) tetracarboxamide phthalocyanine (FeTcaPc) was obtained and dried at 65 °C for 12 h. The mixture of FeTcaPc and 100 mL of concentrated hydrochloric acid was refluxed at 100 °C for 18 h with stirring under N_2 atmosphere. The crude product was filtered and washed several times with deionized water. The obtained filter cake was dissolved in 0.2 M NaOH solution. The solution was adjusted to about pH 2 by adding 3 M HCl solution. The flocculent precipitate began to form and was washed with deionized water until the pH of the filtrate became neutral. The product was finally washed with ethanol and dried at 65 °C for 12 h to obtain blue–violet FeC_4Pc.

2.4 Preparation of the modified ITO electrode

The ITO glass slices were cleaned by sequentially sonicating in acetone, ethanol, and deionized water for 20 min each and dried under infrared lamp prior to use. A homogeneous suspension was prepared by mixing 3 mg of FeC_4Pc and 10 mg of TiO_2 nanoparticles in 1 mL DMSO with the aid of sonication. About 20 μL of the suspension was dropped onto the ITO glass slice and allowed to dry

naturally to form a $FeC_4Pc@TiO_2$/ITO working electrode. FeC_4Pc/ITO, TiO_2/ITO, and ITO working electrodes were obtained using the same method.

2.5 PEC measurements

The PEC detection of HQ was conducted as follows. A certain concentration of HQ was added to the PEC reaction pool containing 4 mL of PB solution (0.1 M, pH=3) at room temperature. and the PEC experiments were performed by chronoamperometry on an electrochemical workstation with potential of 0.7 V under visible LED light irradiation.

3. RESULTS AND DISCUSSION

3.1 Characterization of photoelectric active material

The chemical structure of FeC_4Pc was determined by FTIR and UV-Vis spectra to confirm its successful synthesis. Fig. 1A shows the FTIR spectrum of FeC_4Pc. The characteristic absorption peaks of the carboxy group were observed at 3429 cm^{-1} (O–H stretching vibration), 1716 cm^{-1} (C=O stretching vibration), and 940 cm^{-1} (O–H bending vibration). The absorption peaks at 1611, 1379, 1330, and 736 cm^{-1} are attributed to the vibrations of the phthalocyanine skeleton [38]. As shown in the UV-Vis spectrum (Fig. 1B), the as-synthesized FeC_4Pc exhibits a characteristic Soret band at 334 nm, which is attributed to the $a_{2u}(\pi)$ to $e_g^*(\pi)$ transition. The other characteristic absorbance band in the range of 600–700 nm is due to Q bands corresponding to the $a_{1u}(\pi) - e_g(\pi)$ transition [18]

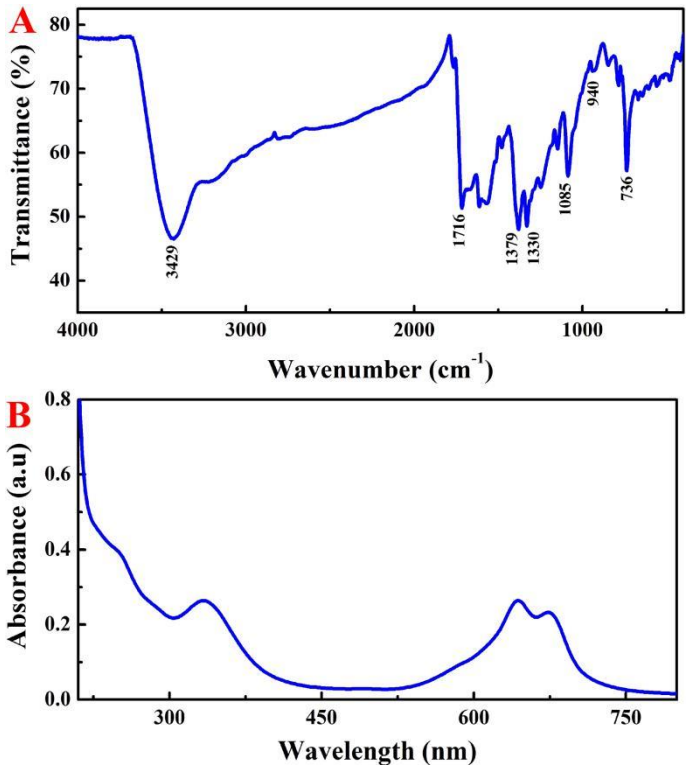

Figure 1. (A) FTIR spectrum and (B) UV-Vis spectrum of FeC_4Pc.

3.2 Characterization of PEC sensor

Electrochemical impedance spectrometry (EIS) studies were performed to characterize the electron transfer process of the modified electrode. Nyquist plots were obtained in 0.1 M KCl solution containing 5 mM $[Fe(CN)_6]^{3-/4-}$ (Fig. 2A). The charge transfer resistance values of FeC_4Pc/ITO and TiO_2/ITO are lower than that of the bare ITO because of their excellent electrical properties. Control experiments were carried out on the $FeC_4Pc@TiO_2$ composite materials and their individual counterparts. The $FeC_4Pc@TiO_2$ composite showed the smallest charge transfer resistance due to the synergistic effect between FeC_4Pc and TiO_2. This property is of great significance for using the photoelectrode in PEC analysis.

The photocurrent response signals of the modified photoelectrodes to 0, 20, and 60 μM HQ were recorded in saturated oxygen solution. The addition of HQ led to an obvious enhancement of the photocurrent signal (Fig. 2B). The $FeC_4Pc@TiO_2$/ITO composite shows a photocurrent about 10-fold higher than ITO, 4-fold higher than FeC_4Pc/ITO, and 3-fold higher than TiO_2/ITO in 0.1 M PB solution containing 60 μM HQ under visible LED light. The $FeC_4Pc@TiO_2$ composite material has higher separation efficiency of the photo-generated electrons and holes and PEC efficiency. Therefore, $FeC_4Pc@TiO_2$/ITO was used as the working electrode for detection of HQ.

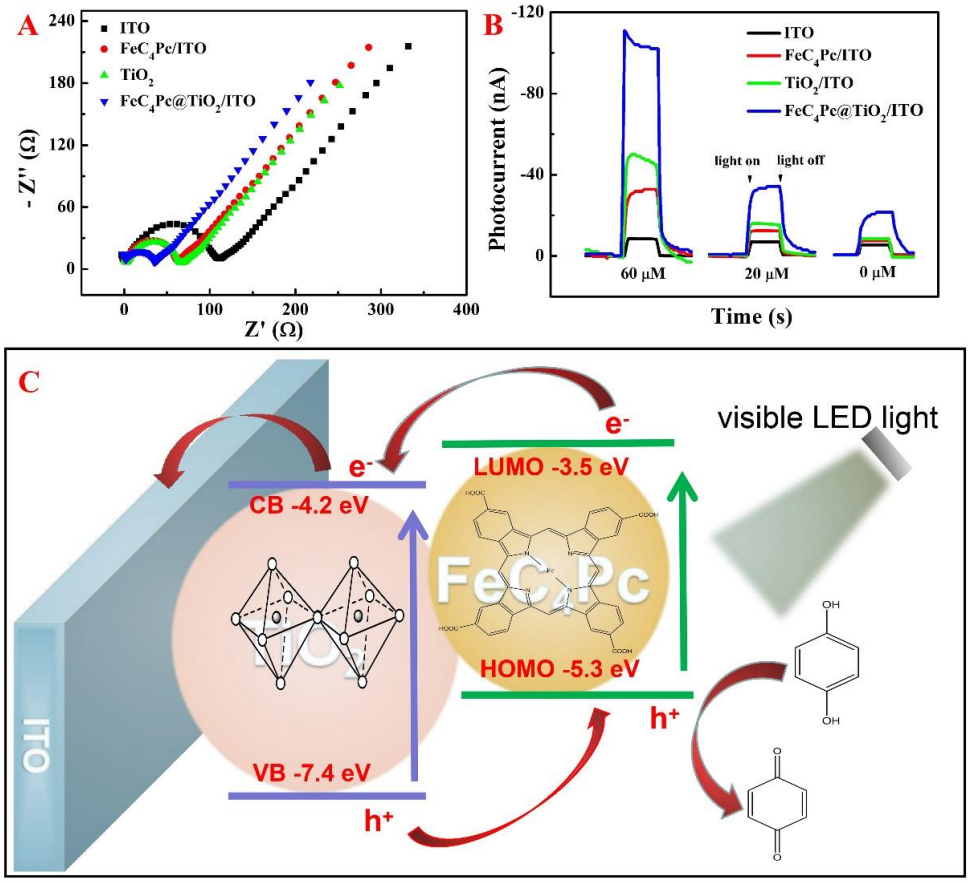

Figure 2. (A) Nyquist plots of the various photoelectrodes in 0.1 M KCl solution containing 5 mM $[Fe(CN)_6]^{3-/4-}$. (B) Photocurrent response of various photoelectrodes in 0.1 M PB solution containing 0, 20, and 60 μM HQ. Proposed mechanism for PEC detection of HQ.

3.3 Possible mechanism of the proposed PEC sensor

Fig. 2C shows the possible mechanism of the proposed PEC sensor for detection of HQ. Under visible LED light irradiation, FeC_4Pc absorbed high photon energy and electrons in the highest occupied molecular orbital (HOMO) were excited and transferred to the lowest unoccupied molecular orbital (LOMO). These photo-generated electrons then transferred to the conduction band (CB) of TiO_2 nanoparticles. The holes were transferred from the valence (VB) band of TiO_2 nanoparticles to FeC_4Pc. When HQ was added to the PB solution, the photo-generated holes were transferred from the VB of ITO to the surface of the photoelectrode and HQ was oxidized to form benzoquinone, thereby increasing the separation efficiency of photo-generated electron–holes and enhancing the photocurrent response signal [36]. Therefore, the enhancement of photocurrent could be used for quantitative detection of HQ.

3.4 Optimization of electrolyte and pH

The effects of pH and buffer solution were investigated to determine the optimal experimental conditions for detection of HQ (Fig. 3). Given that the pH of buffer solution is an important parameter, the PEC responses of HQ on $FeC_4Pc@TiO_2$/ITO were investigated in PB solution with different pH levels ranging from 2.0 to 8.0. The photocurrent response increased from 2.0 to 3.0 and then decreased from 3.0 to 8.0 (Fig. 3A). The photocurrent was also examined in different buffer solutions, namely PBS, Mcllvaine, potassium hydrogen phthalate–hydrochloric acid (PHP-HA), acetic acid–sodium acetate (AC-SA), and citric acid–sodium citrate (CC-SC) buffer solution with pH 3.0. The best performance of the PEC sensor was achieved in PB solution (Fig. 3B). Hence, PB solution with pH=3.0 was chosen for further experiments.

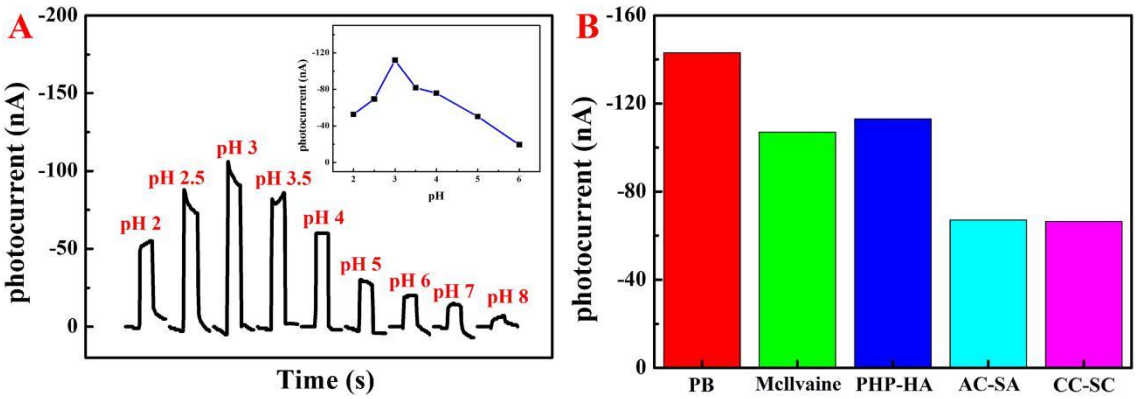

Figure 3. Effect of (A) pH and (B) buffer solution on the photocurrent response to 60 μM HQ.

3.5 PEC detection for HQ

Fig. 4 shows the PEC signals of $FeC_4Pc@TiO_2$/ITO to successive additions of HQ into 0.1 M

PB solution (pH 3.0) under visible LED light. The photocurrent intensity of the PEC sensor increased with increasing HQ concentration in the linear range from 0.2 μM to 78 μM (inset of Fig. 4), with the linear of equation I (nA) = −20.63−1.51C_{HQ} (μM) (r^2 = 0.9981). The limit of detection (LOD) was calculated to be 0.078 μM at a signal-to-noise ratio of 3.

Other studies on HQ sensor are listed in Table 1. The $FeC_4Pc@TiO_2$/ITO electrode exhibited a wider linear range and a relatively low LOD toward HQ compared with other sensors in previous works.

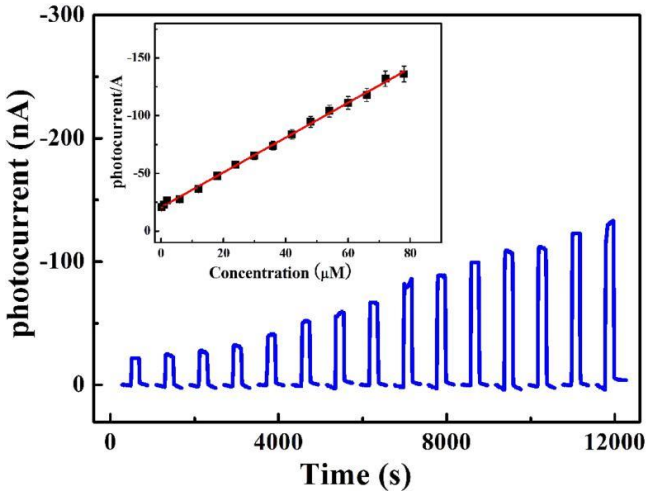

Figure 4. Photocurrent responses of the prepared PEC sensor in 0.1 M PB with successive addition of different concentrations of HQ (range from 0.2 μM to 78 μM). Insert: Analytical curve.

Table 1. Comparison of previous and current HQ detection methods

Electrode material	Detection method	Linear range (μM)	LOD (μM)	Ref.
MoS_2/RGO[a]	DPV[f]	0.001 ~ 0.009	0.0005	35
PS-PNIPAm-PS[b]	DPV	0.6 ~ 2350	0.49	39
Mn-TiO_2 Nanoparticles	CV[g]	2000 ~ 10000	7.5	40
NSCE[c]	Amperometry	50 ~ 500	6.1	41
Gold nanoparticles	Amperometry	0.25 ~ 150	0.1	42
(porphyrin/AuNPs[d]/graphene	Amperometry	0.02 ~ 0.24	0.0046	43
TiO_2/CuCNFs[e]	Amperometry	1 ~ 89.8	3.65	44
$FeC_4Pc@TiO_2$	Amperometry	0.2 ~ 78	0.078	This work

a) reduced graphene oxide; b) poly (styrene-b-(N-isopropylacrylamide)-b-styrene); c) substrate-free nanostructured carbon electrode; d) gold nanoparticles; e) copper and carbon composite nanofibers; f) differential pulse voltammetry; g) cyclic voltammogram

3.6 Stability, reproducibility, and selectivity

The stability of the proposed PEC sensor was investigated. $FeC_4Pc@TiO_2$/ITO was stored in a refrigerator at 4 ℃ for 5 days, and HQ was detected every day under the optimal conditions. The experimental results demonstrated that the photocurrent of the PEC sensor retained 94.87% of the initial photocurrent after 5 days. The reproducibility of the PEC sensor was investigated by five independently conducted parallel experiments with different $FeC_4Pc@TiO_2$/ITO photoelectrodes. The results showed a relative standard deviation (RSD) of -1.20% for photocurrent response signals. This finding implies that the proposed PEC sensor exhibits excellent stability and reproducibility.

The selectivity of the PEC sensor is an important factor that affects its performance. Photocurrent response signals were recorded upon the addition of coexisting inorganic ions and organic compounds including 100-fold Cl^-, SO_4^{2-}, NO_3^-, Na^+, K^+, and urea; 15-fold o-aminophenol; and 10-fold acetaminophen, 3-mercaptopropionic acid, and ascorbic acid. The sensor was considered to be interference-free and showed a change of less than ±5% in the photocurrent response signal before and after the addition of foreign species. As shown in Table 2, the concomitant species had no influence on the detection of HQ. The results demonstrated the sufficient selectivity of the proposed sensor in the PEC detection of HQ.

Table 2. Selectivity of some species for detection of HQ

Foreign species	Molar ratio (foreign species/NP)
Cl^-, SO_4^{2-}, NO_3^-, Na^+, K^+, urea	100
o-aminophenol	15
acetaminophen, 3-Mercaptopropionic acid, ascorbic acid	10

3.7 Detection of HQ in real samples

Table 3. Determination of HQ in river water samples

Sample	Found (μM)	Added (μM)	Amount (μM)	Recovery (%)	RSD (%, n=5)
Fusui	0	20.00	19.97	99.8	1.9
Ningming	0	20.00	20.35	101.7	4.1
Daxin	0	20.00	19.95	99.7	1.9

River water samples from Fusui, Ningming, and Daxin were quantitatively analysed to verify the practical application of $FeC_4Pc@TiO_2$/ITO for PEC detection of HQ. Quantitative recovery tests were conducted by recording the photocurrent signals of the water samples added with accurate

concentrations of HQ. The amounts of HQ were detected by calibration curve method. As shown in Table 3, the recoveries were 99.7%–101.7%. The results indicate that the PEC sensor based on $FeC_4Pc@TiO_2$/ITO is reliable.

4. CONCLUSION

In this work, a visible-light PEC sensor based on $FeC_4Pc@TiO_2$ was successfully fabricated. $FeC_4Pc@TiO_2$ exhibited positive synergistic photoelectrocatalytic effects and effective photo-generated charge separation on the PEC analysis of HQ. Under the optimal experimental conditions, the as-constructed sensor showed satisfactory stability, selectivity, and reproducibility for detection of HQ. In addition, the sensor was used to detect HQ in river water samples and obtained excellent recoveries and RSD values. Thus, the proposed PEC sensor could be a promising analytical tool in the fields of environmental monitoring.

ACKNOWLEDGEMENT
The author acknowledges the Guangxi Science Foundation of China [grant No.2016GXNSFAA380113] for providing support to this work.

References

1. J. Lv, X. Chen, S. Chen, H. Li, H. Deng, *J. Electroanal. Chem*., 842 (2019) 161.
2. J. Peng, Q. Huang, W. Zhuge, Y. Liu, C. Zhang, W. Yang, G. Xiang, *Biosens. Bioelectron*., 106 (2018) 212.
3. R. Wu, G.-C. Fan, L.-P. Jiang, J.-J. Zhu, *ACS Appl. Mater. Inter*., 10 (2018) 4429.
4. P. Yan, D. Jiang, H. Li, J. Bao, L. Xu, J. Qian, C. Chen, J. Xia, *Sensor. Actuat B-Chem*., 279 (2019) 466.
5. X.-X. Shi, X.-Q. Li, X.-P. Wei, J.-P. Li, *Chinese J. Anal. Chem*., 48 (2020) 396.
6. W. Zhuge, X. Li, S. Feng, *Microchem. J.*, 155 (2020) 104726.
7. J. Peng, W. Zhuge, Y. Liu, C. Zhang, W. Yang, Y. Huang, *J. Electrochem. Soc*., 166 (2019) B1612.
8. J. Peng, W. Zhuge, Y. Huang, C. Zhang, W. Huang, *B. Korean Chem. Soc*., 40 (2019) 214.
9. C. Wang, Y. Wang, H. Zhang, H. Deng, X. Xiong, C. Li, W. Li, *Anal. Chim. Acta*, 1090 (2019) 64.
10. Z. Li, W. Dong, X. Du, G. Wen, X. Fan, *Microchem. J*., 152 (2020) 104259.
11. B. Çakroğlu, M. Özacar, *Electroanal.*, 32 (2019) 166.
12. R. Viter, K. Kunene, P. Genys, D. Jevdokimovs, D. Erts, A. Sutka, K. Bisetty, A. Viksna, A. Ramanaviciene, A. Ramanavicius, *Macromol. Chem. Phys*., 221 (2019) 1900232.
13. J. Peng, Q. Huang, Y. Liu, P. Liu, C. Zhang, *Sensor. Actuat. B-Chem*., 294 (2019) 157.
14. Y. Li, Z. Li, W. Ye, S. Zhao, Q. Yang, S. Ma, G. Xiao, G. Liu, Y. Wang, Z. Yue, *Electrochim. Acta*, 295 (2019) 1006.
15. I. Ibrahim, H. N. Lim, N. M. Huang, Z.-T. Jiang, M. Altarawneh, *J. Hazard. Mater*., 391 (2020) 122248.
16. W. Yang, X. Wang, W. Hao, Q. Wu, J. Peng, J. Tu, Y. Cao, *J. Mater. Chem*. B, 8 (2020) 2363.
17. S. Shen, J. Chen, M. Wang, X. Sheng, X. Chen, X. Feng, S. S. Mao, *Progr. Mater. Sci*., 98 (2018) 299.
18. S. Y. Neto, R. de C. S. Luz , F. S. Damos, *Electrochem. Commun*., 62 (2016) 1.
19. K. Virkki, E. Tervola, M. Medel, T. Torres, N. V. Tkachenko, *ACS Omega*, 3 (2018) 4947.

20. B. Guan, J. Yu, S. Guo, S. Yua, S. Han, *Nanoscale Adv*., 2 (2020) 1352.
21. Y. Yao, M. Sun, Z. Zhang, X. Lin, B. Gao, S. Anandan, W. Liu, *Int. J. Hydrogen Energ*., 44 (2019) 9348.
22. K. Sakamoto, E. Ohno, *Prog. Org. Coat*., 31 (1997) 139.
23. J. Mack, N. Kobayash, *Chem. Rev*., 111 (2011) 281.
24. J. Peng, Q. Huang, Y. Liu, F. Liu, C. Zhang, Y. Huang, W. Huang, *J. Chinese Chem. Soc*., 66 (2019) 1311.
25. G. Ekineker, M. Goksel, *Tetrahedron*, 76 (2020) 130878.
26. Z. Fan, L. Fan, S. Shuang, C. Dong, *Talanta*, 189 (2018) 16.
27. S. Y. Neto, R. de C. S. Luz, F. S. Damos, *Electroanal*., 28 (2016) 2087.
28. S. Gorduk, O. Avciata, *Inorg. Chim. Acta*, 471 (2018) 137.
29. F. Yurt, K. Ocakoglu, M. Ince, S. G. Colak, O. Er, H. M. Soylu, C. Gunduz, C. B. Avci, *Chem. Biol. Drug Des.*, 91 (2018) 789.
30. Y. Liu, Y.-M. Wang, W.-Y. Zhu, C.-H. Zhang, H. Tang, J.-H. Jiang, *Anal. Chim. Acta*, 1012 (2018) 60.
31. Sirajuddin, M. I. Bhanger, A. Niaz, A. Shah, A. Rauf, *Talanta*, 72 (2007) 546.
32. T.-S. Chen, S.-Y. Liou, W.-W. Kuo, H.-C. Wu, G.-P. Jong, H.-F. Wang, C.-Y. Shen, V. V. Padma, C.-Y. Huang, Y.-L. Chang, *Luminescence*, 30 (2015) 947.
33. E. Scobbie, J. A. Groves, *Ann. Occup. Hyg*., 43 (1999) 131.
34. K. Jurica1, I. B. Karačonji, S. Šegan, D. M. Opsenica, D. Kremer, *Arh. Hig. Rada Toksiko*., 66 (2015) 197.
35. Y. Peng, Z. Tang, Y. Donga, G. Che, Z. Xin, *J. Electroanal. Chem*., 816 (2018) 38.
36. X. Ma, J. Chen, Y. Wu, S. Devaramani, X. Hu, Q. Niu, C. Zhang, D. Shan, H. Wang, X. Lu, *J. Electroanal. Chem.*, 820 (2018) 123.
37. K. S. Lokesh, A. Adriaens, *Dyes Pigments*, 96 (2013) 269.
38. Y. Wan, Q. Liang, T. Cong, X. Wang, Y. Tao, M. Sun, Z. Li, S. Xu, *RSC Adv*., 5 (2015) 66286.
39. P. Zhao, M. Ni, C. Chen, C. Wang, P. Yang, X. Wang, C. Li, Y. Xie, J. Fei, *Electroanal*., 2020, Early Access, DOI:10.1002/elan.201900644.
40. Z. A. Ansari, T. Athar, H. Fouad, S. G. Ansar, *J. Nanosci. Nanotechno*., 2017, 17, 2296-2301.
41. M. A. Aziz, D. Theleritis, M. O. Al-Shehri, M. I. Ahmed, M. Qamaruddin, A. S. Hakeem, A. Helal, M. A. A. Qasem, *ChemistrySelect*, 2 (2017) 4787.
42. P. Wang, D. Huang, W. Guo, J. Di, *J. Solid State Electr*., 22 (2018) 123.
43. Y. Hu, Z. Xue, H. He, R. Ai, X. Liu, X. Lu, *Biosens. Bioelectron*., 47 (2013) 45.
44. J. Yang, D. Li, J. Fu, F. Huang, Q. Wei, *J. Electroanal. Chem*., 766 (2016) 16.